



A functionally graded cathode for proton-conducting solid oxide fuel cells

Chunli Yang*, Qiming Xu

Postdoctoral Mobile Research Station of Materials Science and Engineering, Xi'an University of Architecture and Technology, Jingzai Road 96, Xi'an, Shanxi 710055, PR China

ARTICLE INFO

Article history:

Received 16 February 2012

Received in revised form

14 March 2012

Accepted 16 March 2012

Available online 13 April 2012

Keywords:

Solid oxide fuel cells

Thermal expansion coefficient

Graded cathode

Thermal cycles

ABSTRACT

The cobalt-containing cathode materials facilitate the activity of oxygen reduction, but they also suffer from problems like high thermal expansion coefficients, which cause poor thermal compatibility with electrolytes and limited performance stability. In this work, a functionally graded $\text{PrBaCo}_2\text{O}_5$ (PBCO) cathode is developed for solid oxide fuel cells (SOFCs) based on proton-conducting $\text{BaCe}_{0.7}\text{Zr}_{0.1}\text{Y}_{0.2}\text{O}_{3-\delta}$ (BCZY) electrolyte. The compositions of the cathodes are gradually changed from a material that is active for oxygen reduction and more compatible with the electrolyte BCZY to another material that is more conductive for current collection. The single cells have high resistance to thermal shock, showing well-combined cathode-electrolyte interface after 60 times of thermal cycles. Meanwhile, a maximum power density of 588 mW cm^{-2} and a low polarization resistance of $0.08 \Omega \text{ cm}^{-2}$ is achieved at 700°C , respectively. The impedance spectra indicate that the optimized cathode structure greatly improves the polarization resistance while ohmic resistance is mainly determined by the conductivity and thickness of electrolyte. The results demonstrate that this configuration not only buffers the TEC mismatch but also optimizes the cathode structure for oxygen reduction reaction.

© 2012 Elsevier B.V. All rights reserved.

1. Introduction

Solid oxide fuel cells (SOFCs) have attracted much attention worldwide because of the demand for clean, secure, and renewable energy [1,2]. Unfortunately, the high operating temperature seriously inhibits long term stability and durability of material systems, which limits broad commercialization [3]. In order to reduce the working temperature, two technical barriers have to be overcome in order for intermediate temperature SOFC performance to be comparable to that in high temperature: high ohmic resistance of electrolyte and relatively low catalytic activity of electrodes, especially cathode under lower temperature range [4].

Since the proton conductors were found by Iwahara et al. [5,6], they have attracted more and more attention because of the advantages such as low activation energy [7] and high energy efficiency [8] compared with conventional oxide-ion conducting electrolytes. Many perovskite-type oxides, particularly the rare earth doped BaCeO_3 oxides which exhibit the highest conductivities have been extensively employed as the electrolytes [9,10]. A major challenge for this type of proton conductors is a proper compromise between conductivity and chemical stability because the samples easily decompose when exposed to a $\text{CO}_2/\text{H}_2\text{O}$ atmosphere in practical environment. By suitable doping, these

materials can obtain both adequate proton conductivity as well as sufficient chemical and thermal stability over a wide range of SOFC operating conditions, e.g., $\text{BaCe}_{0.7}\text{Zr}_{0.1}\text{Y}_{0.2}\text{O}_{3-\delta}$ (BCZY) [11].

The development of proper cathode materials for proton-conducting SOFCs in order to improve materials compatibility and interfacial polarization still remains a challenge. Many cobalt-containing perovskite-type mixed ionic and electronic conductors (MIEC), such as $\text{La}_x\text{Sr}_{1-x}\text{Co}_y\text{Fe}_{1-y}\text{O}_{3-\delta}$ (LSCF) [12], $\text{Ba}_{0.5}\text{Sr}_{0.5}\text{Co}_{0.8}\text{Fe}_{0.2}\text{O}_{3-\delta}$ (BSCF) [13] and $\text{Sm}_{0.5}\text{Sr}_{0.5}\text{CoO}_{3-\delta}$ (SSC) [14], have been extensively studied as cathode materials, which potentially extend three phase boundary (TPB) active region over the entire cathode. Recently layered perovskite oxide $\text{PrBaCo}_2\text{O}_5$ (PBCO) with ordered A-cations has also been extensively investigated as potential cathode material [15–18]. The disorder-free oxygen migration mechanism makes this material exhibit excellent oxygen catalytic activity due to the special crystal structure [19–21]. Unfortunately, these active cobalt-based cathodes in practical long term application often suffer from some disadvantages, in which the high thermal expansion coefficients (TECs) always cause electrolyte–cathode interface delamination resulting in the cell performance dramatic degradation [22,23]. Towards this problem, the strategy commonly adopted to reduce the thermal mismatch is mixing these cathodes with electrolyte material to form composite cathodes, to a certain extent, which narrow the difference of the TEC with that of electrolyte. However, composite cathodes cannot solve this problem completely because the amount of electrolyte material adding into cathode has a limit for maintaining required TPB sites. Furthermore, the increased resistance

* Corresponding author. Tel./fax: +86 29 82205245.

E-mail addresses: clyang@mail.ustc.edu.cn, clyangustc@163.com (C. Yang).

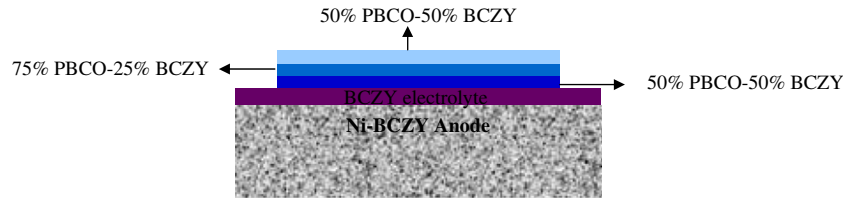


Fig. 1. Schematic diagram of the triple-layer cathode single cell.

of composite cathode will cause large ohmic drop due to weakened ability of current collection [24]. To avoid the undesirable sharp discontinuities in TECs, graded cathodes were developed to join the incompatible components [25,26]. Instead of an abrupt change in composition between two materials, functional graded cathodes have gradient interface at which the composition gradually changes from a catalytically active layer to a current collecting layer. From the view of electrochemical performance, this configuration not only buffers the TEC mismatch but also optimizes the cathode structure for oxygen reduction reaction. To date, however, this optimization design hasn't been applied for proton-conducting SOFCs but can potentially improve the cathode thermal compatibility and electrochemical performance.

In this work, triple-layer graded cathodes based on PBCO layered perovskite were developed for proton-conducting SOFCs with a stable BCZY electrolyte, with very encouraging performance at 600–700 °C. The cathode showed excellent thermal stability

(or thermal shock resistance) without degradation. The microstructure, performance and thermal behavior were investigated.

2. Experimental

The electrolyte $\text{BaCe}_{0.7}\text{Zr}_{0.1}\text{Y}_{0.2}\text{O}_{3-\delta}$ (BCZY) powders were synthesized by Pechini method with citrate and ethylenediamine tetraacetic acid (EDTA) as parallel complexing agents. Y_2O_3 was dissolved in nitric acid first, and stoichiometric amounts of $\text{Ba}(\text{NO}_3)_2 \cdot 9\text{H}_2\text{O}$, $\text{Ce}(\text{NO}_3)_3 \cdot 6\text{H}_2\text{O}$ and $\text{Zr}(\text{NO}_3)_4 \cdot 4\text{H}_2\text{O}$ were dissolved in EDTA- NH_3 aqueous solution under heating and stirring. An appropriate amount of citric acid was added in the solution. The solution was heated under stirring to evaporate water until it converted to viscous gel and finally ignited to flame, obtaining the white ash. The ash was then calcined in air at 1000 °C for 3 h.

A dry-pressing/co-firing method was employed to fabricate the bilayer anode-supported cells. NiO + BCZY + starch mixture (3:2:1

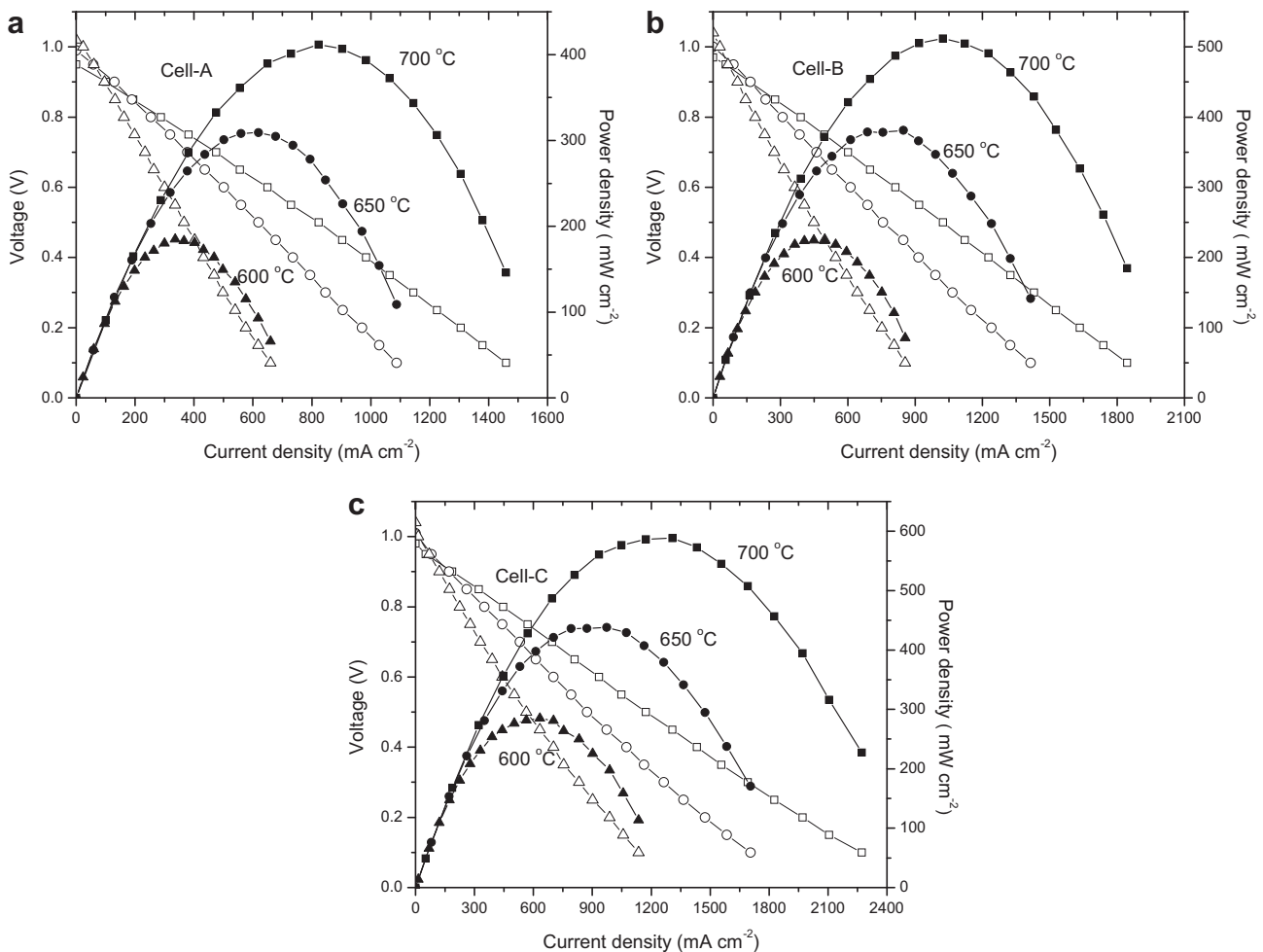


Fig. 2. Performance of the as-prepared cells with hydrogen at different temperatures: (a) cell A; (b) cell B and (c) cell C.

in weight) was pre-pressed at 200 MPa to form an anode substrate. Then the loose BCZY powder was uniformly distributed onto the anode substrate, co-pressed at 250 MPa, and subsequently co-sintered at 1350 °C for 5 h to obtain the bilayer cells of NiO-BCZY/BCZY with dense electrolyte. The $\text{PrBaCo}_2\text{O}_{5+\delta}$ (PBCO) cathode powders synthesized by the same process were calcined at 1000 °C for 3 h. The composite cathode slurries were prepared by mixing BCZY and PBCO in different weight ratio and a 6 wt% ethylcellulose-terpineol binder. Schematically shown in Fig. 1 is the cathode composed of three layers with BCZY content gradually decreased and PBCO content gradually increased in the direction away from the electrolyte–electrode interface. Each of the three individual compositions was coated twice. The graded cathode was finally fired at 1000 °C for 3 h to obtain the cell with functional electrode structure with three layers (briefly cell C). For comparison, the cell with pure PBCO cathode (briefly cell A) and the cell with 50 wt% PBSC:50 wt% BCZY cathode (briefly cell B) were fabricated. The electrode active area was about 0.24 cm².

Electrochemical measurements of single cells (A, B and C) were performed from 600 to 700 °C with humidified hydrogen (~3% H₂O) as fuel and the static air as oxidant. The flow rate of fuel was controlled at 25 sccm. The voltage–current curves were recorded by DC Electronic Load (IT8511) at a scanning rate of 50 mV s⁻¹. AC impedance spectroscopy (Chi604c, Shanghai Chenhua) was performed on the cells under open-circuit conditions. The thermal cycles were carried out by repeating operating temperature from 700 °C to 500 °C then back to 700 °C with heating rate of 10 °C per minute. After every cycle when temperature was back to 700 °C, voltage–current curves and impedance were measured. The total test time lasted about 60 h. Five cells were tested for each kind of cell configuration respectively and the mean cell performances were obtained. A scanning electron microscope (SEM, JSM-6390LA) was used to observe the microstructure of the as-prepared cells and the cells after thermal-cycle test.

3. Results and discussion

3.1. Electrochemical performances

Electrochemical performances of the cell A, B and C with different cathodes in humidified hydrogen were tested to demonstrate the effect of graded cathode on electrochemical performances. As we can see from Fig. 2 that the maximum power density (P_{max}) of cell A with pure PBCO cathode reached 411 mW cm⁻² at 700 °C. For cell B with composite cathode (50wt.% PBCO and 50wt.% BCZY), the P_{max} was improved to 512 mW cm⁻² at 700 °C. The current density at 0.1 V was 1844 mA cm⁻², much higher than that of cell A (1460 mA cm⁻²). For cell C, the P_{max} increased to 588 mW cm⁻² at 700 °C when the three-layer graded cathode was employed. The result could be explained by the improvement of the cathode configuration. The pure PBCO cathode in cell A can only provide mixed oxide-ion and electronic conductivities by its inherent conducting property. When the PBCO cathode is mixed with BCZY, the proton conductivity in cathode will be enhanced, which could essentially increase the reaction TPB, thus promote the cell performance. Furthermore, BCZY could suppress the growth of PBCO grains, thereby maintain the porosity and increase TPB area, creating a greater density of reaction sites in the cathode. Recent studies on composite cathodes for proton-conducting SOFC also demonstrated the improvement of reaction sites by simply mixing the electrolyte material with MIEC cathode [27]. For cell A and B, however, the monolayer cathode is not the best functional architecture to develop the potential power output to full. The composite cathode indeed greatly improved the TPB but also exhibited relatively high sheet resistance, resulting in large ohmic drop due to

that the effect of current collecting is weakened compared with pure PBCO cathode [24]. In cell C, a layer of current collector (pure PBCO) is painted over PBCO-BCZY composite layer. The P_{max} value was elevated to 588 mW cm⁻² at 700 °C. The current density at 0.1 V was also greatly improved from 1460 mA cm⁻² (for cell A) to 2272 mA cm⁻². It is believed that the triple-layer cathode, comprised by gradual changing PBCO and BCZY contents, with the optimized TPB zone for reactions and current collecting layer, fulfilled a structural and functional optimization on configuration. It can be expected that the cell performance will be further improved when the cathode thickness is decreased.

The electrochemical impedance spectra were used to evaluate the cathode polarization resistances, which are shown in Fig. 3. The total electrode polarization resistances can be readily obtained from the difference between the high-frequency and low-frequency intercepts of impedance loop with the real axis. At

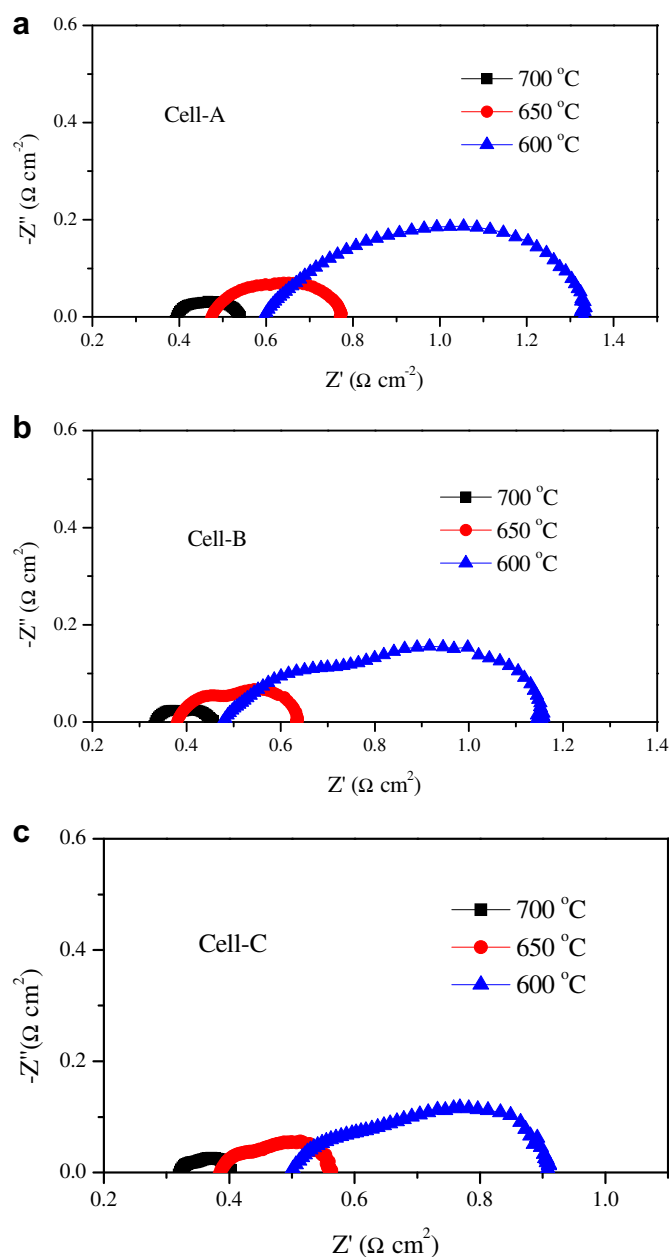


Fig. 3. Impedance spectra of the cells measured under open-circuit conditions at different temperature: (a) cell A; (b) cell B and (c) cell C.

650 °C, the electrode polarization resistances of cell A, B and C were 0.3, 0.25, and 0.18 $\Omega \text{ cm}^2$, respectively. Since the cells had the same anode–electrolyte interface, the difference in electrode polarization resistance must attribute to different cathode polarization behaviors. The PBCO-BCZY based functionally graded cathodes with a composition changed from a catalytically active layer to a current layer effectively promote the oxygen reduction reaction proceeding in the more reasonable way. Hence, the cathode polarization resistances were greatly improved in cell C, and compared to cell A, the value was reduced by 46.7% at 700 °C, 40% at 650 °C and 44.6% at 600 °C, respectively. The ohmic resistance of the cell A, B and C was 0.59, 0.48 and 0.5 $\Omega \text{ cm}^2$, respectively. The cell ohmic resistances are composed of those of anode, electrolyte, cathode and interfacial resistances of anode–electrolyte and cathode–electrolyte provided the contact series resistances are neglected. The cells had the same compositions of 0.7 mm anode substrate, 20 μm electrolyte membranes but different cathode layers and cathode–electrolyte interfaces. The cell A showed the highest ohmic resistance of 0.59 $\Omega \text{ cm}^2$. For cell B and C, the values were improved to

0.48 $\Omega \text{ cm}^2$ and 0.5 $\Omega \text{ cm}^2$. This might be resulted from the interfacial environment of cathode–electrolyte during cathode sintering process. The mismatch of TECs between pure PBCO and electrolyte BCZY in cell A might cause tiny delamination in cell fabrication process. Obviously, the cell B with composite cathode having close TEC with electrolyte inhibits this condition. For cell C, the configured three-layer cathode has the lowest extent of TEC mismatch, but the thickness of cathode layer ($\sim 60 \mu\text{m}$) was greater than that of cell B ($\sim 20 \mu\text{m}$) due to the fabrication limitation. Therefore, cell C showed a little greater ohmic resistance than that of cell B at the same operating temperatures.

3.2. Thermal stability and microstructure of graded cathodes

The thermal cycles test were carried out to investigate the ability of cathodes against thermal shock. The operating temperature was designed to cool to 500 °C at 10 °C min^{-1} then rise back to 700 °C at the same rate for measurements, accounted as one cycle. Fig. 4 shows the impedance of cell A, B and C after different thermal cycles. As we can see, the ohmic resistance of cell A increased by 10.3% after 60 cycles, indicating that the cathode–electrolyte interfaces deteriorate during repeated heating–cooling process. The electrode polarization resistance greatly increased by 53.3% in cell A, which can be observed by both high-frequency arc and low-frequency arc increasing as cycle times. Consequently, the P_{max} rapidly decreased from 441 mW cm^{-2} before cycles to 331 mW cm^{-2} (Fig. 5). To elucidate the origin of the cell performance degradation, the microstructures of post-test cells were shown in Fig. 6. As shown in Fig. 6(a), after firing at 1000 °C for 3 h in air, the pure PBCO cathode of cell A can well adhere to the electrolyte. After the thermal cycles for 60 times, the obvious delamination appeared with a gap of 10 μm , which could be always observed along the cathode–electrolyte interface layer (Fig. 6(b)). As a cobalt-containing cathode, the TEC of PBCO is as high as $24.6 \times 10^{-6} \text{ K}^{-1}$ [28]. The great internal lattice expansion and contraction in PBCO differing from that of BCZY would lead to increasing the stresses of the ceramic bonding between cathode layer and electrolyte induced by any change of thermal environment. Therefore, the rapid heating cycles and cooling cycles in the test process undoubtedly aggravated the delamination situation, which directly leads to the increases of ohmic resistance and cathode polarization resistance as mentioned above.

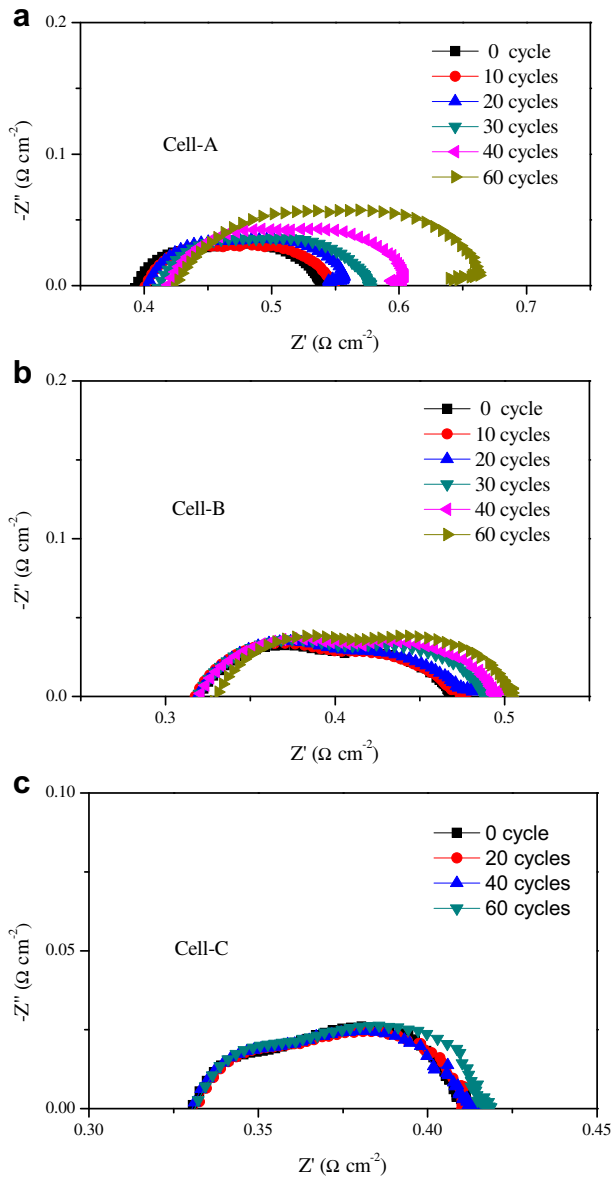


Fig. 4. The impedance of cell A, B and C after different thermal cycles.

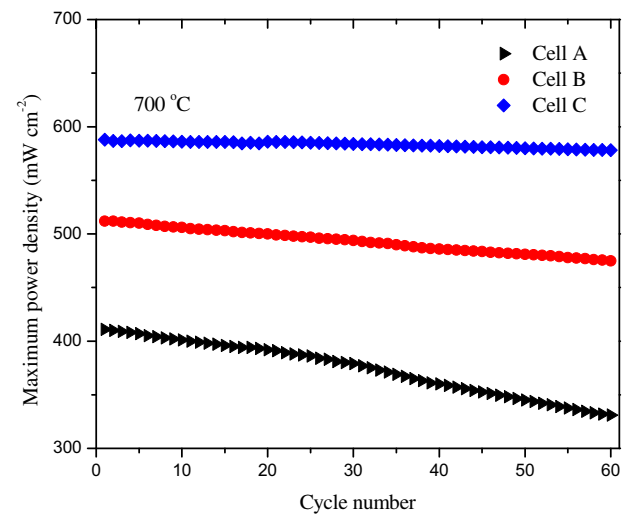


Fig. 5. The maximum power density (P_{max}) of the cells at 700 °C as a function of the thermal cycles.

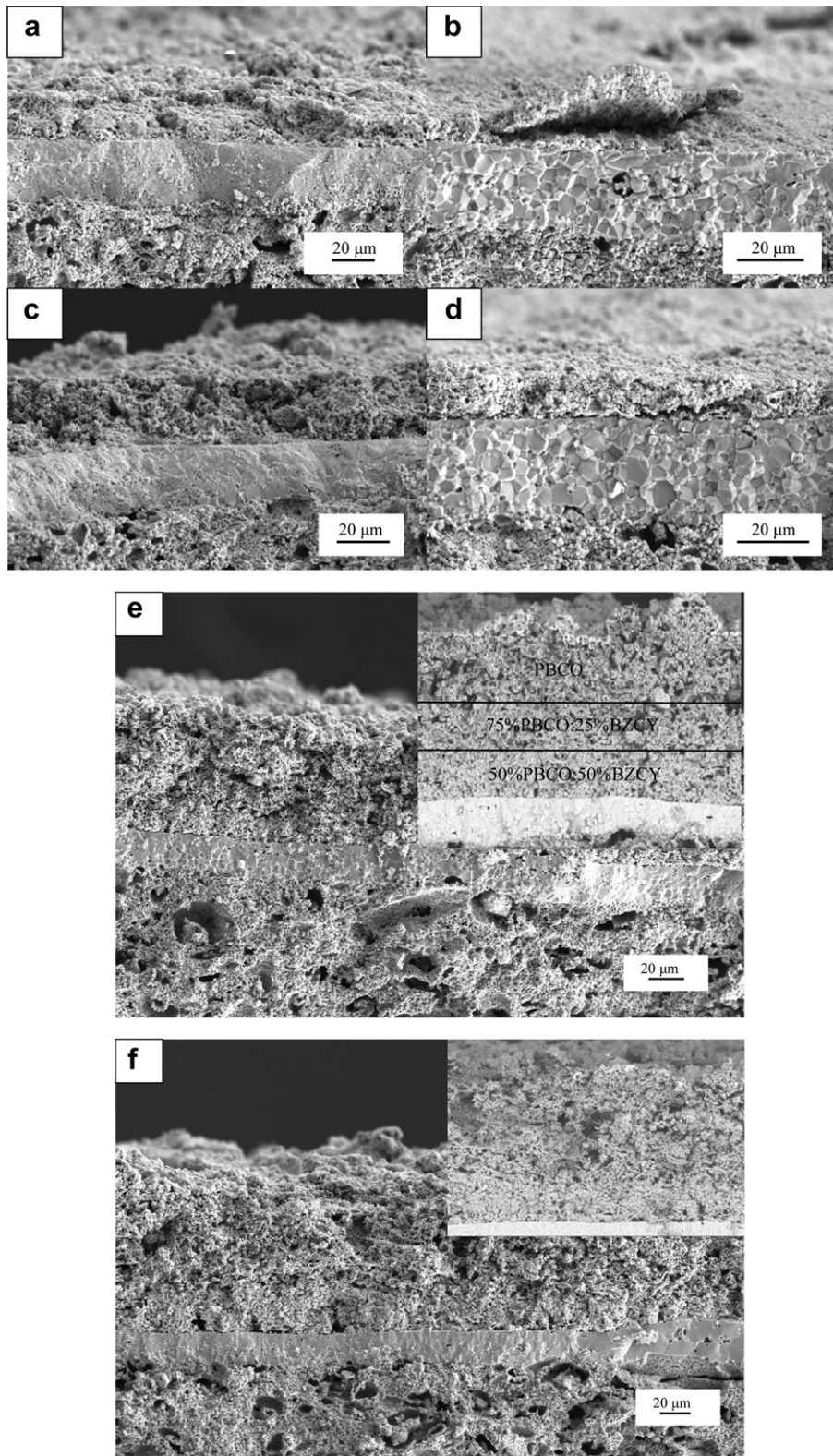


Fig. 6. Comparison of electrolyte-cathode interfaces of cell A (a), B (c) and C (e) before thermal-cycle testing and cell A (b), B (d) and C (f) after the test.

In cell B, the addition of BCZY into cathode (50% PBCO and 50% BCZY in weight) improved the TEC mismatch to some extent. The ohmic resistance and electrode polarization resistance increased slowly as cycling times. After 60 cycles, the resistances rose up by

6.45% and 13.3%, respectively. The P_{\max} also slowly decreased from 512 mW cm^{-2} before cycles to 475 mW cm^{-2} . It is believed that the addition of BCZY narrowed the difference of TECs between the electrolyte and fabricated composite cathode. From Fig. 6(c) and

(d), we can see the interface was greatly improved, just some tiny cracks with narrow gap channels in limited area between PBCO and BCZY. The BCZY ceramic particles in the cathode constituted rigid network bones with similar TEC to the dense BCZY film. Consequently, the expansion caused by PBCO can be effectively inhibited by the strong bonding between the BCZY ceramic bones and the electrolyte.

In cell C with a graded cathode, there was no observable change in impedance spectra. The power density is very stable after 60 cycling times, only 1.7% degradation in P_{\max} . Fig. 6(e) and (f) show the cross-section views of the cell C with three layers functionally graded PBCO cathode before and after the electrochemical test and thermal cycle test. The individual layer adhered to adjacent layer pretty well without fracture, indicating the inter-layers strain was negligible. The bottom layer is the composite of 50 wt% PBCO and 50 wt% BCZY, which plays a critical role in oxygen reduction and H–O reaction as TPB reaction area. The middle layer of 75wt% PBCO and 25wt% BCZY is employed to buffer the TEC mismatch between the bottom layer and top layer. Meanwhile, this layer with more PBCO phase is also beneficial to conduction of electrons from top layer to bottom TPB layer where majority of oxygen reduction reaction occurs. As mixed ionic–electronic conductor of PBCO, partial oxygen reduction also takes place above the electrolyte–cathode interface, while the produced oxygen ions are transported to TPB through PBCO bulk. The top layer is pure PBCO cathode which buffers the strain from lower two layers. This porous three-layer assembly as a whole was integrated into a well-combined thermal-resistant buffer zone, adhering to electrolyte pretty well without any cracks after thermal cycles. The results demonstrated the functional graded cathode with TEC transition effectively buffers the thermal stress in all interfacing layers. In this configuration, it should be noted that the top layer of pure PBCO also plays an important role as collection layer, which substitutes noble metal and simultaneously improve the liability of cell system. In practical experimental works, silver paste has been often used as current collection by painting very thin film on top of the cathode. However, thermal incompatibility and weak bonding between silver film and cathode usually cause serious crack, which consequently results in the sharp performance degradation, especially under thermal shock conditions. As reported by Liu et al., the electrical conductivity of PBCO exhibited as high as 240 S cm^{-1} at $600 \text{ }^\circ\text{C}$, showing the potential to be a current collector without most commonly used silver or platinum [18]. In addition, the gradient TEC in the whole cathode structure makes PBCO current collector strongly endure severe practical operating conditions.

4. Conclusions

In order to promote the thermal stability of cell performance, a functionally graded PBCO cathode was developed for solid oxide fuel cells (SOFCs) based on $\text{BaCe}_{0.7}\text{Zr}_{0.1}\text{Y}_{0.2}\text{O}_{3-\delta}$ (BCZY) electrolyte.

The compositions of the cathodes are gradually changed from a material that is active for oxygen reduction and more compatible with the electrolyte BCZY to another material that is more conductive for current collection. By comparison and analysis, the assembly cells have high resistance to thermal shock with well-combined cathode–electrolyte interface after 60 times of rapid thermal cycles. A maximum power density of 588 mW cm^{-2} and a low polarization resistance of $0.08 \text{ } \Omega \text{ cm}^2$ was achieved at $700 \text{ }^\circ\text{C}$, respectively. The impedance results indicate that the optimized cathode structure significantly improved the polarization resistance due to the proper assembly of different functional layers. The results demonstrate that this configuration not only buffers the TEC mismatch but also optimizes the cathode structure for oxygen reduction reaction.

Acknowledgment

This research was supported by the Basic Research Foundation of Xi'an University of Architecture and Technology (No. JC1107)

References

- [1] D. Brett, A. Atkinson, N. Brandon, S. Skinner, *Chem. Soc. Rev.* 37 (2008) 1568.
- [2] A.J. Jacobson, *Chem. Mater.* 22 (2010) 660.
- [3] B.C.H. Steele, A. Heinzel, *Nature* 414 (2001) 45.
- [4] H. Ding, X. Xue, *J. Power Sources* 195 (2010) 4139.
- [5] H. Iwahara, T. Esaka, H. Uchida, N. Maeda, *Solid State Ionics* 3/4 (1981) 359.
- [6] H. Iwahara, H. Uchida, K. Ono, K. Ogaki, *J. Electrochem. Soc.* 135 (1988) 529.
- [7] A.F. Sammells, R.L. Cook, J.H. White, J.J. Osborne, R.C. MacDuff, *Solid State Ionics* 52 (1992) 111.
- [8] A.K. Demin, P.E. Tsiakaras, V.A. Sobyanyan, S.Y. Hramova, *Solid State Ionics* 152–153 (2002) 555.
- [9] T. Higuchi, T. Tsukamoto, H. Matsumoto, T. Shimura, K. Yashiro, T. Kawada, J. Mizusaki, S. Shin, T. Hattori, *Solid State Ionics* 176 (2005) 2967.
- [10] Q. Ma, R. Peng, Y. Lin, J. Gao, G. Meng, *J. Power Sources* 161 (2006) 95.
- [11] C. Zuo, S. Zha, M. Liu, M. Hatano, M. Uchiyama, *Adv. Mater.* 18 (2006) 3318.
- [12] E.P. Murray, M.J. Sever, S.A. Barnett, *Solid State Ionics* 148 (2002) 27.
- [13] Z. Shao, S.M. Haile, *Nature* 431 (2004) 170.
- [14] C. Xia, W. Rauch, F. Chen, M. Liu, *Solid State Ionics* 149 (2002) 11.
- [15] A. Maignan, C. Martin, D. Pelloquin, N. Nguyen, B. Raveau, *J. Solid State Chem.* 142 (1999) 247.
- [16] A. Taskin, A. Lavrov, Y. Ando, *Appl. Phys. Lett.* 86 (2005) 091910.
- [17] J. Kim, A. Manthiram, *J. Electrochem. Soc.* 155 (2008) B385.
- [18] L. Zhao, B. He, B. Lin, H. Ding, S. Wang, Y. Ling, R. Peng, G. Meng, X. Liu, *J. Power Sources* 194 (2009) 835.
- [19] G. Kim, S. Wang, A.J. Jacobson, L. Reimus, P. Brodersen, C.A. Mims, *J. Mater. Chem.* 17 (2007) 2500.
- [20] G. Kim, S. Wang, A.J. Jacobson, Z. Yuan, W. Donner, C.L. Chen, L. Reimus, P. Brodersen, C. A. Mims, 88 (2006) 024103.
- [21] X. Zhang, M. Jin, *J. Power Sources* 21 (2010) 1076.
- [22] B. Wei, Z. Lu, X. Huang, Z. Liu, *J. Am. Ceram. Soc.* 90 (2007) 3364.
- [23] L. Zhao, B. He, Q. Nian, Z. Xun, R. Peng, G. Meng, X. Liu, *J. Power Sources* 194 (2009) 291.
- [24] S. Zha, Y. Zhang, M. Liu, *Solid State Ionics* 176 (2005) 25.
- [25] N. Hart, N. Brandon, M. Day, N. Lapeña-Rey, *J. Power Sources* 106 (2002) 42.
- [26] H. Song, S. Lee, D. Lee, H. Kim, S. Hyun, J. Kim, J. Moon, *J. Power Sources* 195 (2010) 2628.
- [27] B. Lin, H. Ding, Y. Dong, S. Wang, X. Zhang, D. Fang, G. Meng, *J. Power Sources* 186 (2009) 58.
- [28] L. Zhao, J. Shen, B. He, F. Chen, C. Xia, *Int. J. Hydrogen Energy* 36 (2011) 3658.